Simulation of Interfacial Metal Electrodeposition: The Electrochemical Model and the Numerical Implementation

Vassili S. Sochnikov and Shlomo Efrima*

Department of Chemistry and the Ilse Katz Center for Meso and Nanoscale Science and Technology, Ben-Gurion Universty of the Negev, P.O. Box 653, Beer-Sheva, Israel

Received: July 3, 2002; In Final Form: August 19, 2002

We present a detailed physical and numerical model describing electrochemical behavior, aimed eventually at following the shape evolution in interfacial growth (electrodeposition in particular). Details of the numerical implementation are outlined, followed by a few telling examples of the electrochemical behavior at thin disk electrodes and at thick cylindrical electrodes. We demonstrate the large effect that radial mass transport has in the case of practically stationary thin electrodes, and the unusual behavior of propagating thin electrodes.

1. Introduction

In the past decade or so, metal electrodeposition has been investigated as an attractive model system for the study of the evolution of morphology in growth processes of propagating surfaces and boundaries.[1] Electrochemical deposition offers an easily controllable and varied set of experimental conditions and system parameters, together with convenient time scales and easily measurable system characteristics.[2] These important features were put to use in recent years for the study of growth/form relationships,[3−12] mostly in two-dimensional or laterally thin cell configurations.

In general, electrochemical (metal) deposition is a subject of theoretical and experimental interest, both for its technological importance[13] as well as for its basic scientific challenge.[14] The understanding of electrochemical processes at (practically stationary) electrodes and the microscopic mechanisms governing the voltage/current characteristics have been developed in the past to a high level.[15] However, this strong theoretical and experimental basis is not sufficient when a rapidly growing system (such as a thin interfacial electrodeposit) is considered, when one cannot assume (implicitly or explicitly) quasi-static conditions.[16−17]

Interfacial, essentially 2-D, metal deposition differs from 3-D deposition in a major way, by virtue of the possibility of forming extremely thin deposits (down to a few nanometers), while the lateral dimension can be macroscopically large. This unique geometry is at the core of the appearance of instabilities that affect both the electrochemical characteristics (current/voltage relations, for example) as well as the morphology of the deposit. The extremely thin deposit enables it to grow laterally at unusually high speeds, which strongly affects all the electrochemical behavior.

Past and recent theoretical treatments of electrochemical growth address mainly two-dimensional systems and are mostly based on computer simulations, which take into account both the instantaneous system parameters as well as their preceding history.[18] These simulations can be roughly classified according to the size scale they consider. Most simulations address the submicroscale, starting from an atomistic picture with an atomic size nucleus,[19] which evolves to the size of several nanometers.[20] These numerical renderings rely heavily on "particle" simulation techniques such as Monte Carlo,[21] cellular automata,[22] and, specifically, diffusion-limited aggregation,[23] with the size of the "particles" varying from several angstroms to a few nanometers. A very realistic representation of growth is achieved, though the results and the conclusions are limited to the nanoscale regime.

The other major type of numerical simulation considers large-scale, macroscopic systems and approaches.[12,24−26] Here one does not follow the individual particles, with currents and fluxes being used instead. These macroscopic methods are highly successful within their limited spatial and temporal resolution.

Stability analysis has been used[27] and applied to electrochemical systems.[28−31] The prediction of the large-scale evolution of boundary instabilities was found to be in good correlation with experiments and provided a theoretical framework for the morphology diagrams of electrochemical systems.[1,16,32]

However, on one hand, those simulations do not provide the full connection between the emergence of instabilities and their large scale (typically mm) manifestation, and, on the other hand, they often lack a detailed physical chemical (electrochemical) description combined with the boundary evolution. The general character, as well as the detailed features of a macroscopic shape, are often determined and controlled by the small-scale, high-resolution processes. Processes on the submicro (and even atomistic) level are at the root of the macroscopic forms. Instabilities make it highly nontrivial to extrapolate from the micro to the macro world, making the micromechanism/macroshape relationship complex. It was also widely demonstrated experimentally that large-scale boundary evolution in electrochemistry might be highly complex and requires more extensive and detailed models than the available ones.

In our current work we develop simulations of essentially two-dimensional, interfacial metal electrodeposition, which allows one to carry out simulations over a large range of resolutions, going in principle all the way from the nanoscale up to macroscopic dimensions. Though we explicitly address here the case of interfacial electrodeposition, which leads to two-dimensional morphologies,[16] the technique is general and can be extended to various (both 2- and 3-D) electrochemical systems of interest. A novel approach of treating the interfacial process and its coupling to the propagation of the boundary allows to observe the detailed electrochemical behavior in the system. The numerical framework we developed for the

10.1021/jp026436d CCC: $22.00
Published on Web 10/22/2002

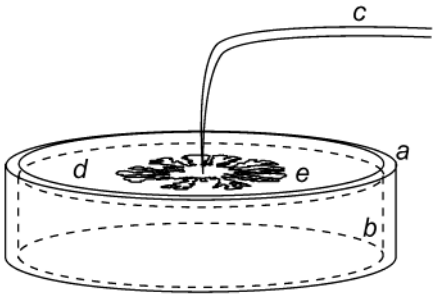

Figure 1. Sketch of the system under consideration: (*a*) circular cell; (*b*) band anode, at the circumference of the cell; (*c*) initial tip cathode; (*d*) solution; (*e*) thin interfacial cathodic growth.

simulations[34] permits the treatment of size scales ranging over several orders of magnitude within a single simulation, and makes efficient use of the computational resources.

In this paper we begin by presenting the physical model and relate it to two-dimensional experiments of metal electrodeposition. Next we describe in detail the numerical implementation of the model. Finally we present results for the spatial and temporal development of the electric current, the voltage, and the concentrations of ions in the system. These results are calculated mainly for establishing the validity of the simulation by comparing it to (theoretically and experimentally) known electrochemical behavior of real electrochemical systems, with stationary, nonpropagating electrodes. A few results for propagating systems will be shown in order to demonstrate the large effect growth has on the electrochemical characteristics.

2. The Electrochemical Model

2.1. Model Description. This simulation focuses on a "thin-electrode" system.[1,2,6,11,12,14,16,17] A circular cell (Figure 1, *a*) contains a circular band counter electrode (Figure 1, *b*) (anode) at its circumference, and a point working electrode (Figure 1, *c*) (the cathode) just touching the silver nitrate solution (Figure 1, *d*) at the dead center of the cell. Experiments show that in such a system silver electrodeposition, as an example, results in a thin deposit (Figure 1, *e*) forming on the surface of the liquid.[16] Typically, within seconds, a deposit is produced[11,16] that is a few nanometers thick (at its center) and a few centimeters wide. This extremely large aspect ratio $\sim 10^6$:1[11,16] justifies a (quasi-) two-dimensional simulation of the system. However, the simulation we propose is more general and can also treat a thick electrode (with a thickness comparable to the depth of the solution), as long as the system is predominately uniform along the depth of the cell. Considering only two-dimensions has a significant advantage over the full (3-D) calculation in terms of computer resources (time and memory), allowing one to invest more efforts in improving the physical model.

Our model addresses three main parts of the system: the cathode, where the deposition takes place, the solution, and the anode. We start the simulation with a seed cathode of a predefined shape (analytically derived or given digitally). The size of the seed is taken to be much larger than the pixel-size of the numerical grid used to digitize space, in order to avoid difficulties arising from the discrete nature of the grid.[34] Only cathodic processes are permitted, no dissolution of the working electrode is allowed. As experiments are usually carried out at large overvoltages, neglecting the anodic contribution on the central working electrode is valid. We can easily relax this condition, when required.

The anode is considered to be inert. We only introduce near it the same amount of ions that are deposited on the cathode, to conserve neutrality and mass. In any event, in real systems, the anode is sufficiently large and distant from the cathode to have any noticeable effect on the overall behavior (except when it releases ions that might "poison" the cathodic deposition, giving rise to the Hecker effect,[35] which we do not consider here, though it can easily be incorporated in the simulation).

The solution contains a given initial concentration of a salt with an electrochemically reactive ion (silver cations), and, optionally, a supporting electrolyte. There are no restrictions on the concentrations of any of the salts, and they can be chosen at will to suit any specific system of interest. Realistic diffusion coefficients and mobility of the various ions are used.

Potentiostatic conditions are assumed in a two-electrode system, with a constant potential. The potential of the anode is the reference potential (i.e., its potential is taken to be zero). The overvoltage is evaluated from the potential of the cathode, V, combined with the reversible redox potential of the electrochemical reaction, $E_R = E_0 - (RT/nF)\ln[Ag^+]$, (for silver reduction $E_0 = 0.799$ V) and the absolute potential of the hydrogen evolution reaction, $E_H = 4.310$ V.[36]

$$\eta = V - E_R + E_H \tag{1}$$

From the computational point of view we divide space into cells within a square grid. The grid is hierarchical, consisting of cells of varying sizes, so as to give the best resolution near the cathode and use less computer resources deep in the solution. This grid is adaptive, in the sense that it readjusts itself to the propagating cathodic deposit.[34] Each "pixel" (cell or vertex on the grid) of our discreet representation of the system can be either the cathode or the anode, or the solution. To each cell in solution we attribute a set of concentrations and an electric potential (the latter being constant for the cells holding the cathode and anode). At each step of the evolution of the system the values of the concentrations and of the potential are reevaluated.

As stated above, we impose potentiostatic conditions by setting the cathode potential at a fixed negative value (typically of a few volts), with the anode kept at 0 V. The distribution of the electric potential φ throughout the "solution" is determined by solving the Laplace equation,[37] eq 2.

$$\nabla^2\varphi = 0 \tag{2}$$

At present, the hierarchical grid that the simulation uses is feasibly limited to 10−12 "generations",[34] i.e. grid cell sizes ranging between 1 cm and 2.5 μm, thus eliminating the need to solve the Poisson[37] (or the Boltzmann−Poisson[15]) equations. Electroneutrality is assumed by the use of the Laplace equation (and imposed algorithmically everywhere and at all times). When finer details are of interest (grid cell sizes down to ~10 nm), the Boltzmann−Poisson equation should replace the Laplace equation, giving also double layer effects.

Equation 2 is solved iteratively. The iterations are continued until the largest difference of the potential for any grid cell between two consecutive iterations falls below the required precision (typically below 1.0 μV). As we shall see, the main potential drop, and the main changes in the potential with time, occur near the cathode. Thus we obtain a precision better than 1.0 μV (typically $<10^{-4}$ % of the voltages considered here) in a region of space characterized by potential gradients of ~1 V over a few grid cells (representing a few microns in actual size). This level of precision is adequate for our needs.

The boundary conditions for eq 2 need to be specified at the electrodes. The two-dimensionality of the calculation makes it unnecessary to treat the solution−air (or cell wall) surface explicitly. The precise boundary conditions at the anode are not really important, as all the interesting events in metal electrodeposition occur near the cathode. We simply impose a value of 0 V at all the points adjacent to the anode.

The boundary conditions near the cathode are extremely important and are determined by requiring at each point along its surface the equality of the local migration current[38] (eq 3) and the current passing through the cathode surface, as given by the Butler−Volmer equation[15] (eq 4)

$$i_{\mathrm{mig}} = (F^2/RT)\,\Sigma_j z_j^2 D_j C_j \nabla\varphi \tag{3}$$

$$i_{\mathrm{BV}} = i_{\mathrm{o}} C_{\mathrm{r}}(x,y)/C_{\mathrm{ro}}\,[\exp(\eta/b_{\mathrm{a}}') - \exp(-\eta/b_{\mathrm{c}}')] \tag{4}$$

where i is the current density (A cm^{-2}) calculated from the migration (i_{mig}) and Butler−Volmer (i_{BV}) expressions, z_j is the charge of the ion j (including the ions of the supporting electrolyte, if present). F is the Faraday constant (C mole^{-1}), R is the universal gas constant (J mole^{-1} K^{-1}), T is the temperature (K), D_j is the diffusion coefficient of species j (cm^2 sec^{-1}), C_j is the concentration of ion j (mole cm^{-3}), $C_{\mathrm{r}}(x,y)$ denotes the instantaneous concentration of the reactive ions at the point (x,y), whereas the sum is over all the types of ions in the system. i_{o} is the exchange current density (A cm^{-2}) determined at a concentration C_{ro}, η is the overvoltage (V), and b_{a}' and b_{c}' are the Tafel slopes (V) for the anodic and cathodic processes, respectively, divided by ln10.

The boundary value of the potential at each point adjacent to the cathode is obtained by solving eq 3 with respect to the potential iteratively subject to eq 4. We usually require the equality of the two currents to be at least within 0.1% at any of the surface points. Equation 4 requires that eq 2 is also solved simultaneously, to obtain the potential drop in the solution cells next to the cathode, used in eq 3. Equation 4 also needs, as input, the instantaneous value of all the concentrations in the various cells. Thus it depends on the history of the system. The calculation of the boundary potential is repeated at each time step with the most recent concentration profiles and size and shape of the cathode. The calculation of the boundary conditions is the most time-consuming stage in the simulation, as it involves the simultaneous solution of equations 2−4 with eq 2. It might take 80 to 100 steps (for an initial convergence or after drastic changes occur), or 10 to 30 steps or less if the system did not deviate too far from its previous state. Figure 2 presents an example of the potential distribution (including the cathode/solution interfacial drop) for the case of a thin circular disk electrode.

Concentration changes for each species, j, present in solution are carried out by means of the diffusion and the migration fluxes (J_{D} and J_{M}, respectively) entering and exiting each computational area element, as given by eq 5 (Fick's law[15]) and eq 6,[38] respectively.

$$J_{\mathrm{D}j} = D_j \nabla C_j \tag{5}$$

$$J_{\mathrm{M}j} = (z_j F/RT) D_j C_j \nabla\varphi \tag{6}$$

These equations are valid only for the solution cells in the computational grid.

At the boundaries we use Faraday's law,[1,15] eq 7, to consume the reactive ions (silver ions, for instance) in the solution cells adjacent to the cathode and to advance the electrode accordingly.

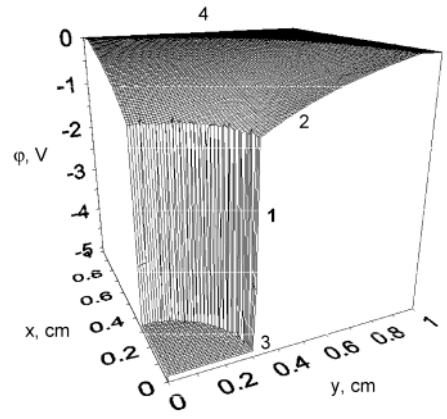

Figure 2. Potential distribution for a circular disk electrode: (1) potential drop at the cathode/solution interface; (2) potential drop in solution; (3) cathode; (4) anode. Only a quarter of the system is shown.

The same total amount of ions is reintroduced uniformly at the anode side of the electrochemical cell, mimicking the dissolution of the anode. This is not mandatory, and can be omitted, to simulate the case of an anodic process that does not involve the metal ions (electrolysis of the solvent, for instance)

$$\Delta l = -\,i\,M_{\mathrm{r}}/(zF\rho)\,\Delta t \tag{7}$$

where Δl is the propagation of the electrode at any given point (cm) over the time interval Δt (s); M_{r} is molar weight of the reactive species (g mol^{-1}), and ρ is the density of the cathode (g cm^{-3}).

The boundary conditions we implement were used for cases of macroscale morphology simulations,[26,39] and the treatment of the concentration fields as outlined above is well established in electrochemical simulations.[9,14,24,25,40]

Using the ion transport equations (eq 5 and 6) to move ions between the grid cells often slightly disrupts electroneutrality. Therefore, following each step of varying the potential and then the concentrations, we impose electroneutrality in each cell. The charge difference between adjacent cells is calculated and then minimized by moving ions between those cells according to the ion transport numbers. This usually involves a very small correction, which does not have any significant effect on the actual concentrations of the various ions in the computational cells.

The physical growth of the cathode via the metal deposition is an important feature of the simulation, being most important when morphology becomes of prime interest. The amount of ions deposited at each time step during the evolution of the system, and at each point of the boundary, is given by Faraday's law, eq 7.

The consumption of the ions near the cathode (and their introduction at the anode) creates concentration gradients near the electrodes, in addition to the electric potential gradients. Both gradients are responsible for driving the reactive ions toward the cathode, and their specific nature determines the shape of the deposit, as well as the electrochemical behavior.

To avoid unphysical situations that might develop during the simulation (such as negative concentrations), to prevent large oscillations, and to comply with the requirements of the level set algorithm, we restrict the time interval at each time step of the simulation. The simulations use the smallest time step obtained from the following three criteria: (*i*) neither consumption of the reactive ions (as calculated from Faraday's law) nor

diffusion/migration of any species in solution should exceed some predefined relative threshold (typically the smaller of either 1% of the initial concentration of that given ion or 1% of its current amount in the cell from which this ion is moved or consumed); and (*ii*) the growth of any cell in any time step should not exceed a value prescribed by the level set stability limitations[41] (typically less than one mesh unit of the grid).

The model we propose is by no means restricted to all the aspects described above. We already pointed out that there is no inherent need to reintroduce the reactive ions at the anode. Similarly, the Laplace equation used to solve for the spatial distribution of the electric potential can be replaced by the Poisson−Boltzmann equation, provided that the time scale of propagation is much longer than the time scale for ion equilibration (which is usually the case, especially when a supporting electrolyte is present). This introduces double layer effects, which are important for very high resolution simulations. In that case, neutrality does not need to be imposed on the system.

In addition, one can allow for a nonuniform potential distribution in the cathode itself, as might be the case for highly convoluted morphologies when variations of the resistance of the cathode are significant. The simulation can also be shifted down to smaller dimensions (for instance, to the range 10 nm to 50 μm) if one wants to focus on these scales. A shift to smaller, atomistic scales is possible but requires replacing the diffusion and migration equations with their microscopic (molecular dynamics or Monte Carlo) analogues, introducing fluctuations in the small volume (area) elements and definitely using the Poisson−Boltzmann equation instead of the Laplace equation. One could also extend our present approach to galvanostatic conditions, which are of interest in various experiments.[42]

2.1. The Numerical Implementation. Implementing the physical model described above within a dynamic hierarchical and adaptive grid framework[34] requires special care, since the resolution may vary from cell to cell. Special precise methods are needed near the working electrode, where topological changes occur with (area) solution elements turning into cathode elements (with entirely different variables) and where one encounters vector-represented quantities (such as the electric current). Solving the Laplace equation (eq 1) utilizes a nonuniform four-points stencil,[43] with explicit treatment of every distance from its center to the neighbors.

The concentration profile calculations are carried out in terms of fluxes entering and exiting all cells. Exchange between up to eight neighbors is considered, to minimize the orientation-dependent influence of the underlying grid,[44] especially near the boundary. Each neighbor is treated separately in such a manner that the different intercell distances (stemming from different scales of resolution) are taken into account automatically.

Addressing cells near the cathode, where the vector-represented current is obtained on the basis of the spatial distribution of the concentration and the potential, requires very special attention. For this purpose we consider each cell with a boundary passing through it to be fully within the cathode. Then we calculate the normal to the surface going through such a surface cell. The closest cell along this normal, which is completely within the solution (i.e., holds no boundary elements within it), provides the concentration and potential variables at that point of the surface. See Figure 3 for a schematic representation of this approach.

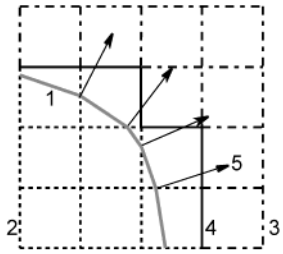

Figure 3. Schematic representation of the cathode/solution interface: (1) the boundary as it is represented by the level set method;[41] (2) cells that fully belong to the cathode (dotted line); (3) cells that are fully in solution (dash−dotted lines); (4) the border between boundary cells (solid line); (5) normals from the points of intersection of the level set boundary and the grid lines pointing to the solution cell from which physical quantities are extracted.

To avoid numerical difficulties dimensionless quantities are used:

$$C_{\text{norm}} = C_i/C_{i,o} \tag{8}$$

$$\varphi_{\text{norm}} = \varphi_i/b' \tag{9}$$

where $C_{i,o}$ is the initial concentration for ion of type.

3. Numerical Results−A Circular Static Electrode Test Case. As a test of the simulation, we now present the results for a few cases of electrochemical behavior for which both theoretical and experimental results are known. The model was coded using C++ and has been run on a variety of platforms (x86, Sun, Compaq, Macintosh, SGI). A detailed discussion of the computational aspects of the simulation is presented elsewhere,[34] while here we focus on the electrochemical behavior.

To establish the validity of our calculation, we first consider a thick circular silver electrode (the thickness of which is equal to that of solution), simulating the well-known case of a cylindrical electrode located in a cylindrical cell.[15] Its growth turns out to be so slow as to be practically negligible through out the relevant time of the calculation. This electrode is immersed into a silver nitrate aqueous solution with an optional supporting electrolyte (NH_4NO_3), and potentiostatic conditions are applied. The anode is also made of silver and dissolves releasing silver ions into the solution, without changing its shape and size. A typical concentration of silver nitrate is 5×10^{-2} M,[16] that of the supporting electrolyte is 5×10^{-1} M, the exchange current density is 1.9×10^{-1} A cm^{-2},[45] and the Tafel slope is 5.1×10^{-2} V.[45]

The current−voltage dependence[46] calculated with the potential applied across the cell ranging between 3.53 and 3.83 V (0.02V − 0.32 V, in terms of overvoltage) is presented in Figure 4 and agrees with the expected behavior of reaching a limiting value of the current (here reached at an overvoltage of 0.2 V). Diffusion control sets in shortly after we "turn on" the potential as shown by the behavior of the concentration near the cathode in Figure 5. The corresponding current−time dependence is presented in Figure 6. Both concentration and current decrease continuously until they reach some potential-independent limiting value. After that, further decreases are still apparent, but at a much lower rate (as expected for unstirred solutions). This behavior is in good agreement with what has been seen in experiments and predicted from theory.[15] The value of overvoltage applied to the system was set so that under any value of the exchange current density (see eq 4 and Figure 8) the system would reach the mass transport limit.

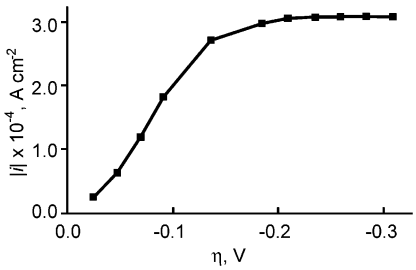

Figure 4. Current density (averaged over the circumference of the circular electrode) as a function of overvoltage. System setup: thick stationary electrode; solution composed of $AgNO_3$ (0.05 M) and NH_4NO_3 (0.5 M). Squares represent calculated values connected with interpolated lines.

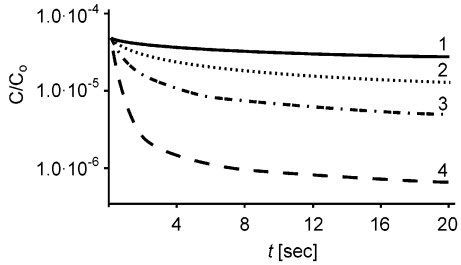

Figure 5. Concentration of silver ions near the cathode (averaged over the circumference of a cylindrical circular electrode) as a function of time for several overvoltages: (1) −0.1 V; (2) −0.15 V; (3) −0.2 V; (4) −0.3 V. The solution holds $AgNO_3$ (0.05 M) and NH_4NO_3 (0.5 M).

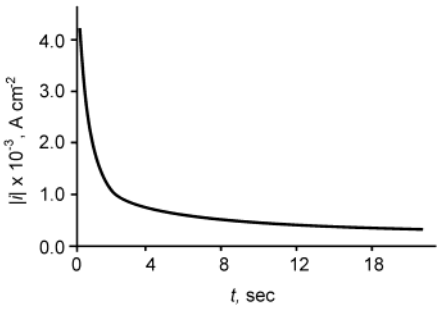

Figure 6. Current density (averaged over the circumference of a cylindrical electrode) as a function of time. The solution holds $AgNO_3$ (0.05 M) and NH_4NO_3 (0.5 M). The overvoltage is 1.4891 V.

The initial concentration of the silver nitrate hardly affects the time dependence of the current (Figure 7). The small deviations of the concentration-normalized curves from each other stem from the faster depletion of the silver ions in the solution when the concentrations are lower (a faster growing diffusion layer). Similarly we find that the limiting value of the concentration near the cathode is proportional to the concentration.

Changing the value of the exchange current density (Figure 8) and that of the Tafel slope (Figure 9) does not affect the limiting diffusion-controlled current and concentration themselves (though this affects the initial time dependence), as expected.[15,46] For larger exchange currents the limiting values are reached slightly faster, which is expected on the basis of the faster electrodic reaction in these cases. The effect of the change of the Tafel slope in this respect is smaller. These results demonstrate the reliability of the simulation and show that it captures the correct electrochemical behavior.

The next step is to apply this simulation framework for the investigation of thin, two-dimensional metal electrodeposits on the surface of solutions or in laterally thin cells. Unlike the case

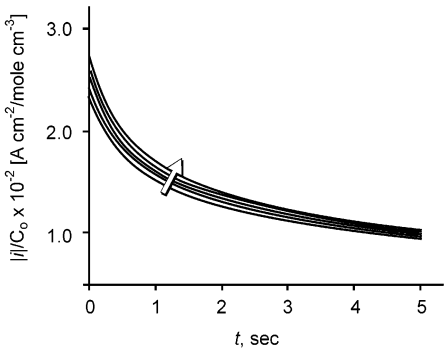

Figure 7. Current density (averaged over the circumference of a cylindrical electrode) divided by the bulk concentration of the reactive ion as a function of time for different concentrations. The arrow shows the direction of increasing C_o from 5×10^{-4} to 5 M (in factors of 10). The solution holds $AgNO_3$ only (no supporting electrolyte). The total cell voltage is 5 V, and the overvoltage is 1.4891 V.

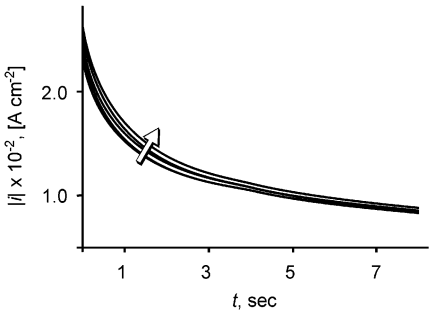

Figure 8. Current density (averaged over the circumference a cylindrical electrode) as a function of time for different values of the exchange current density. The arrow shows the direction of increasing exchange current density value from 1.9×10^{-3} to 19 A (in factors of 10). The solution is composed of $AgNO_3$ (0.05 M). The total cell voltage is 5 V, and the overvoltage is 1.4891 V.

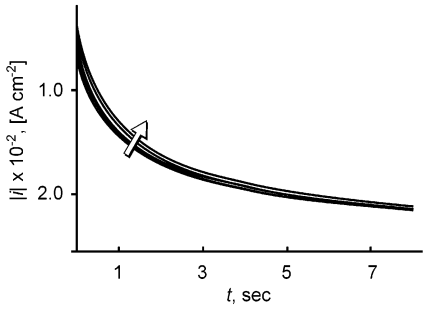

Figure 9. Current density (averaged over the circumference of a cylindrical electrode) as a function of time for different values of the Tafel slope. The arrow shows the direction of decreasing Tafel slope value from 0.203 to 0.025 V (in factors of 2). The solution is composed of $AgNO_3$ (0.05 M). The total cell voltage is 5 V, and the overvoltage is 1.4891 V.

of a bulk cylindrical electrode, a nanometer thin electrode exhibits fast growth, with the deposit edging quickly toward the anode. This, together with radial mass transport, bring about uncommon behavior in terms of the potential, the current, and the concentration their spatial distribution and temporal evolution. This behavior is covered in full detail in a separate future paper. Here we present a few results, to demonstrate the interesting electrochemical behavior that is exhibited by propagating boundaries in the two-dimensional configuration.

Figure 10 top shows the time-dependence of the concentration of the reactive metal ions near the cathode for various overpotentials, for a growing 1 nm thick deposit. We compare it to a similar thin electrode under the same conditions (composition

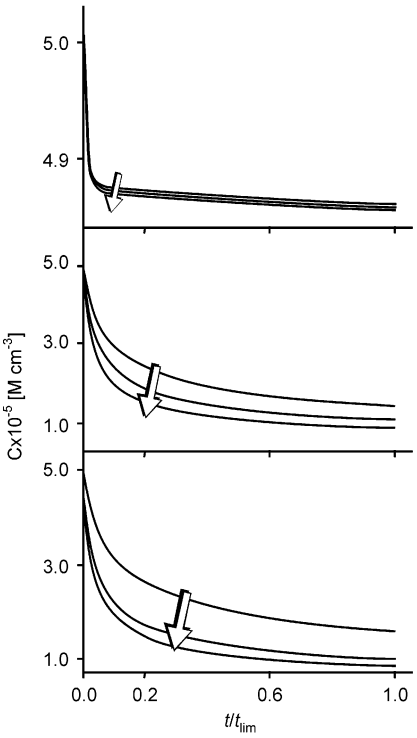

Figure 10. Concentration of silver ions (averaged over the circumference of the electrode) as a function of time for different voltages. The arrow shows the direction of increasing overvoltage from 1.489 to 3.489 V (in intervals of 1 V). Top−thin growing electrode (numerical oscillations were smeared out); middle−thin stationary electrode; bottom−thick stationary electrode. The solution is composed of 0.05 M $AgNO_3$. The time is normalized to that required to reach the limiting conditions as observed, for instance, in Figures 6−9.

of solution and potential applied to the system), which is artificially prevented from growing (by using an appropriate switch in the computer program, Figure 10 middle). While the thin stationary electrode behaves qualitatively in much the same way as the cylindrical electrode shown in (Figure 10 bottom), the concentration near the growing electrode behaves very differently. The concentration hardly decreases at all, maintaining a high value, close to that of the bulk value, at all times. The advancing deposit sweeps through virgin ion-rich regions, which have not yet been exhausted to any significant amount. The stationary electrodes, in contrast, exhaust the ions in their vicinity, and these are replenished only to a limited degree by diffusion (and migration). Also, the dependence on the overvoltage of the advancing electrode is significantly different than that of the stationary electrodes. In the former case the concentration near the electrode practically does not depend on the potential, while in the latter cases higher overpotential leads to a faster and larger decrease in the concentration of the reactive ions. Note also that the currents, Figure 11, are much higher for the thin electrodes, compared to the cylindrical one. The stationary thin electrode benefits from radial diffusion, which brings in a larger flux of ions, compared to the essentially linear diffusion of the bulk electrode. The growing deposit, in addition to the radial diffusion, and actually much more importantly, simply "visits" virgin regions of a high metal ion concentration, leading to exceptionally large currents. Also, the dependence of the current on the overvoltage is vastly different for these three cases, as will be presented in detail in a subsequent report.

Simulations such as those described above require extensive computer resources to achieve a realistic presentation of the physical system under study here. A typical full-scale calculation

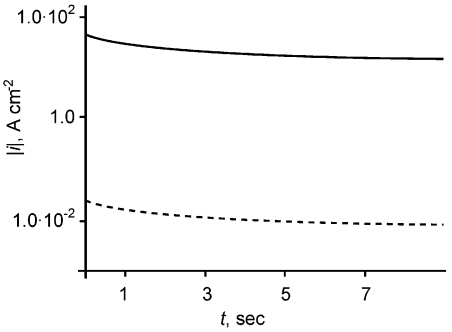

Figure 11. Current density (averaged over the circumference of the electrode) as a function of time for thin (solid line) and thick (dashed line) electrodes. The solution is composed of $AgNO_3$ (0.05 M). The total cell voltage is 5 V, and the overvoltage is 1.4891 V.

of a propagating thin electrode takes approximately 1 h to 1 day on a PC (dual PIII 800 MHz). The time required depends on the precise system parameters (the electric potential, the concentration of the reactive ions, the presence of a supporting electrolyte and its concentration, etc). In a previous report, our simulation compared favorably with other (nonelectrochemical) simulations that propagate boundaries.[34] It is difficult to find other full-scale electrochemical simulations to which one can compare the efficiency of our approach. Suffice it to say that a full simulation can be obtained within a conveniently accessible time of modern PC computers.

Conclusions

We presented an efficient simulation approach for electrodeposition that reliably simulates all the aspects of electrochemical behavior. Though it is designed specifically for predominately two-dimensional cases, it can also be applied directly to cases where the third dimension retains the same projected 2-D shape (i.e., a cylindrical electrode immersed in a cylindrical cell). It accounts for the electric potentials, the ion concentrations, and the (evolving) shape of the metal electrodeposits, and can calculate all the important electrochemical variables (such as currents) as a function of time. The extension to a full 3-D calculation is also possible.

We demonstrated the reliability of the simulation by comparing to a "classical" case of a cylindrical electrode. We also showed first results for the effect two-dimensionality has on the electrochemical behavior. In particular, a very significant effect of the motion of the growing thin electrode on the concentrations and currents was observed.

Acknowledgment. We acknowledge partial support from the Israel Academy of Science and from the Intel Corp., Israel. We acknowledge helpful discussions with M. Deutsch and the work of O. Younes at past early stages of this work.

References and Notes

(1) Saguès, F.; Lopez-Salvans, M. Q.; Claret, J. *Phys. Rep.* **2000**, *337*, 97.

(2) Chazalveil, J.-N.; Rosso, M.; Chassaing, E.; Fleury, V. *J. Electroanal. Chem.* **1996**, *407*, 61.

(3) Matsushita, M.; Hakayama, Y.; Sawada, Y. *Phys. Rev. A* **1985**, *32*, 3814.

(4) Stanley, H. E.; N. Ostrowsky, N. *On growth and form. Fractal and non-fractal patterns in physics*; Martinus Nijhoff Publishers.: Dordrecht, 1988.

(5) Stanley, H. E.; N. Ostrowsky, N. *Random fluctuations and pattern growth: experiments and models*; Kluwer Academic Press: Dordrecht, 1988.

(6) Chazalveil, J.-N. *Phys. Rev. A* **1990**, *42*, 7355.

(7) Bunde, A.; Havlin, S. *Fractals and disordered systems*; Springer-Verlag.: Berlin, 1991.
(8) Vicsek, T. *Fractal growth phenomena*; World Scientific: Singapore, 1992.
(9) Barkey, D.; Garik, P.; Ben-Jacob, E.; Miller, B.; Orr, B. *J. Electrochem. Soc*. **1992**, *139*, 1044.
(10) Couyet, J.-F. *Physics and fractal structure*; Masson, Springer: Paris, 1996.
(11) Zeiri, L.; Younes, O.; Efrima, S.; Deutsch, M. *Phys. Rev. Let*. **1997**, *79*, 4685.
(12) Elezgaray, J.; Lėger, C.; Argoul, F. *Phys. Rev. Let*. **2000**, *84*, 3129.
(13) David, J. *Nature* **2002**, *436*, 716.
(14) Lėger, C.; Servant, L.; Brunnel, J. L.; Argoul, F. *Physica A* **1999**, *263*, 305.
(15) Bockris, J. O'M; Yager, E. B. *Comprehensive treatise of electrochemistry*; Plenum Press: New York, 1980.
(16) Zeiri, L.; Younes, O.; Efrima, S. *J. Phys. Chem. B* **1997**, *101*, 9299.
(17) Lėger, C.; Elezgaray, J.; Argoul, F. *Phys. Rev. E* **1998**, *58*, 7700.
(18) Nicolis, G.; Prigogin, I. *Exploring complexity: an introduction*; W. H. Freeman: New York, 1989.
(19) Voss, R. F.; Tomkiewicz, M. *J. Electrochem. Soc*. **1985**, *132*, 371.
(20) Roberts, A. P.; Knackstedt M. A. *Phys. Rev. E* **1993**, *47*, 2724.
(21) Kalos, M. H.; Whitlock, P. A. *Monte Carlo methods*; J. Wiley & Sons: New York, 1986.
(22) Wolfram, S. *Theory and applications of cellular automata*; World Scientific: Singapore, 1986.
(23) Meaking, P. *Fractal, scaling and growth far from equilibrium*; Cambridge University Press: Cambridge, 1998.
(24) Fleury, V.; Chazalveil, J.-N.; Rosso M. *Phys. Rev. Let*. **1992**, *68*, 2492.
(25) Marshall, P.; Mocakos, P.; Swinney, H. L.; Huth, J. M. *Phys. Rev. E*. **1999**, *59*, 2157.
(26) Prentice, G. A.; Tobias, C. W. *J. Electrochem. Soc*. **1982**, *129*, 78.
(27) Mullins, W. W.; Sekerka, J. *J. Appl. Phys*. **1963**, *34*, 323.
(28) Sunderström, L.-G.; Bark, F. H. *Electrochem. Acta* **1995**, *40*, 599.
(29) Halsey, T. C. *Phys. Rev. A*. **1987**, *36*, 3512.
(30) Barkey, D. P.; Muller, R. H.; Tobias, C. W. *J. Electrochem. Soc.* **1989**, *136*, 2207.
(31) Grier, D. G.; Kessler, D. A.; Sander, L. M. *Phys. Rev. Lett*. **1987**, *59*, 2315.
(32) Ravaine, S.; Breton, C.; Mingotaud, C.; Argoul, F. *Mater. Sci. Eng. C*. **1999**, *8*−*9*, 437.
(33) Grier, D.; Ben-Jacob, E.; Clarke, R.; Sander, L. M. *Phys. Rev. Lett.* **1986**, *56*, 1264.
(34) Sochnikov, V.; Efrima S. *Int. J. Numer. Methods Eng.* **2002**, accepted for publication.
(35) Younes, O.; Zeiri, L.; Efrima, S. *Langmuir* **1997**, *13*, 1767.
(36) Trassat, S. *J. Electrochem. Soc*. **1974**, *52*, 313.
(37) Morse, P.; Feshbach, H. *Methods of theoretical physics*; McGraw-Hill: New York, 1953.
(38) Bockris, J. O'M.; Reddy, A. K. N. *Modern electrochemistry*; Plenum Press: New York, 1970.
(39) Subramanian, V. R.; White, R. E. *J. Electrochem. Soc*. **2000**, *147*, 1636.
(40) Bonnefont, A.; Argoul, F.; Bazant, M. Z. *J. Electroanal. Chem.* **2001**, *500*, 52.
(41) Sethian, J. A. *Level set methods and fast marching methods*; Cambridge University Press: Cambridge, 1999.
(42) Huth, J. M.; Swinney, H. L.; McCormic, W. D.; Kuhn, A.; Argoul, F. *Phys. Rev. E* **1995**, *51*, 3444.
(43) Lau, C.-J. *Applied numerical methods for partial differential equations*; Prentice Hall: Singapore, 1994.
(44) Juric, D.; Tryggvason, G. *J. Comput. Phys*. **1996**, *132*, 127.
(45) Bard, A. J. *Encyclopedia of electrochemistry of the elements*; M. Dekker Inc.: New York, 1973.
(46) Gileadi, E. *Electrode kinetics for chemists, chemical engineers, and material scientists*, VCH: New York, 1993.